

Near-infrared quantum cutting in Ce^{3+} , Yb^{3+} co-doped YBO_3 phosphors by cooperative energy transfer

JinDeng Chen^a, Hai Guo^{a,b,*}, ZhengQuan Li^a, Hao Zhang^a, YiXi Zhuang^b

^a Department of Physics, Zhejiang Normal University, Jinhua, Zhejiang 321004, PR China

^b State Key Laboratory of Silicon Materials, Zhejiang University, Hangzhou 310027, PR China

ARTICLE INFO

Article history:

Received 4 August 2009

Received in revised form 18 November 2009

Accepted 31 January 2010

Available online 7 March 2010

Keywords:

Quantum cutting

Cooperative energy transfer

Downconversion

Ce^{3+} , Yb^{3+} co-doped YBO_3

ABSTRACT

An efficient near-infrared (NIR) quantum cutting (QC) in Ce^{3+} , Yb^{3+} co-doped YBO_3 phosphors has been demonstrated, which involves the emission of two low-energy NIR photons (around 973 nm) from an absorbed ultra-violet (UV) photon at 358 nm via a cooperative energy transfer (CET) from Ce^{3+} to Yb^{3+} ions. Yb^{3+} concentration dependent quantum efficiency has been calculated and the maximum efficiency approaches up to 175% before reaching the critical concentration quenching threshold. The development of NIR QC Ce^{3+} , Yb^{3+} co-doped phosphors may open up a new approach to achieve high efficiency silicon-based solar cells by means of downconversion.

© 2010 Elsevier B.V. All rights reserved.

1. Introduction

The high energy of the vacuum ultra-violet (VUV) photons makes it theoretically possible to generate two visible photons for a single absorbed VUV photon with quantum efficiency (QE) close to 200%. This kind of two-photon luminescence phenomenon is called quantum cutting (QC). The visible quantum cutting has received considerable attentions due to its wide application in mercury-free fluorescent lamps and plasma display panels [1].

Interestingly, quantum cutting materials also show promising applications in silicon-based solar cells [2–11]. One major energy loss in Si solar cells is thermalization, which is expected to be considerably reduced if the absorbed ultra-violet (UV)/blue photon ($300 \text{ nm} < \lambda < 500 \text{ nm}$) can be cut into two near-infrared (NIR) photons and then absorbed by Si ($\lambda_{\text{abs}} < 1100 \text{ nm}$). This scheme can possibly be realized by using a rare earth doped quantum cutting phosphor as a downconversion convertor in front of solar cell panels.

Trupke et al. proposed a method to realize multiple electron-hole pair generation per incident photon by downconversion mechanism [12]. From then on, the Tb^{3+} , Yb^{3+} co-doped QC phosphors had been investigated extensively in recent years [2–11]. Vergeer et al. reported QC by cooperative energy transfer

(CET) in $\text{Yb}_x\text{Y}_{0.99-x}\text{PO}_4:\text{Tb}^{3+}$ phosphors [2], which showed an optimal QE of 188% with the doping concentration of Yb^{3+} as high as 99%.

Hitherto, though the physics of CET allows for the efficient QC and the theoretical QE is high [10], the visible emission of Tb^{3+} remains strong and the NIR luminescence of Yb^{3+} is still inevitably weak. These two phenomena resulted from the following reasons. One is the actual QE is low, another is the excitation of the Tb^{3+} is inefficient for its intra-4f forbidden transitions, i.e., low absorption cross sections, typically in the order of 10^{-21} cm^2 [8], the other is the excitation is fixed at individual wavelengths such as 308 nm, 360 nm and 489 nm. Furthermore, the upconversion process of Tb^{3+} excited by energy transfer from Yb^{3+} (excited by NIR 980 nm laser) in Tb^{3+} , Yb^{3+} co-doped system [9], that is so-called back energy transfer, is efficient. All these reasons mentioned above will reduce the usefulness of Tb^{3+} , Yb^{3+} co-doped QC phosphors in silicon-based solar cells.

The Ce^{3+} , Yb^{3+} co-doped QC phosphors may be superior to Tb^{3+} , Yb^{3+} co-doped ones in silicon-based solar cells. First, the absorption of Ce^{3+} is originated from the allowed electric-dipole transition from the 4f ground state to the 5d excited one, which results in a very high absorption cross section in an order of 10^{-18} cm^2 in the UV region [8]. Second, the excitation band of Ce^{3+} is broad and the excitation wavelength of Ce^{3+} can be tuned by the host materials, which means that high QE may be obtained by choosing appropriate host materials. Moreover, the back energy

* Corresponding author. Address: Department of Physics, Zhejiang Normal University, Jinhua, Zhejiang 321004, PR China. Tel.: +86 579 82298570.

E-mail address: ghh@zjnu.cn (H. Guo).

transfer from Yb^{3+} to Ce^{3+} is small. Though the qualities of Ce^{3+} , Yb^{3+} co-doped QC phosphors exceed those of Tb^{3+} , Yb^{3+} co-doped ones, the investigation on the Ce^{3+} , Yb^{3+} co-doped QC phosphors is very scarce [8].

In this work, we demonstrate the NIR QC in Ce^{3+} , Yb^{3+} co-doped YBO_3 phosphors by CET for the first time. The NIR emission around 973 nm, originated from Yb^{3+} : ${}^2\text{F}_{5/2} \rightarrow {}^2\text{F}_{7/2}$ transition, is observed under the excitation of Ce^{3+} : $4f \rightarrow 5d$ absorption (326–377 nm), owing to the CET from one Ce^{3+} ion to two nearest neighboring Yb^{3+} ions simultaneously. The dependence of Yb^{3+} concentration on the visible and NIR emissions, decay lifetime of Ce^{3+} , and QE from the QC phosphors have been investigated. The highest QE approaches 175% before reaching the critical concentration quenching threshold. These results show the development of NIR QC Ce^{3+} , Yb^{3+} co-doped phosphors may open up a new approach to achieve high efficiency silicon-based solar cells by means of downconversion.

2. Experimental

Powder samples of $\text{YBO}_3:\text{Ce}^{3+}$, Yb^{3+} were synthesized by conventional solid-state reaction method. Y_2O_3 (99.99%), $\text{Ce}(\text{NO}_3)_3$ (A.R.), Yb_2O_3 (99.99%), HBO_3 (A.R.) and HNO_3 (A.R.) were used as raw materials. Yb_2O_3 was first dissolved in dilute HNO_3 to prepare $\text{Yb}(\text{NO}_3)_3$ solution (1 M). The mixtures of Y_2O_3 , HBO_3 (10% excess), $\text{Ce}(\text{NO}_3)_3$ (1 M) and $\text{Yb}(\text{NO}_3)_3$ were ground and then heated at 500 °C for 2 h. After cooling to room temperature, the powders were reground and then heated at 900 °C for another 2 h. This process repeated at 1200 °C to make sure that the reaction has been completed and pure $\text{YBO}_3:\text{Ce}^{3+}$, Yb^{3+} has been obtained. The optimum doping concentration of Ce^{3+} and heating temperature were 1% and 1200 °C, respectively. In this paper, the doping concentrations of Ce^{3+} was fixed to 1%, while the Yb^{3+} concentration varied from 0%, 0.2%, 0.4%, 1%, 2%, 3%, 4% to 6%.

X-ray diffraction was carried out on a Philips X'Pert PRO SUPER X-ray diffraction apparatus with $\text{Cu K}\alpha$ radiation ($\lambda = 0.154056$ nm). The emission spectra, excitation spectra, and decay curves were recorded by using a FLS920 spectrofluorometer (Edinburgh Instruments). Emission and excitation measurements were performed by using a 450 W Xe lamp as the excitation source. Decay curves measurements were obtained by using a nanosecond flash-lamp (nF900) as the excitation source. All the measurements were operated at room temperature.

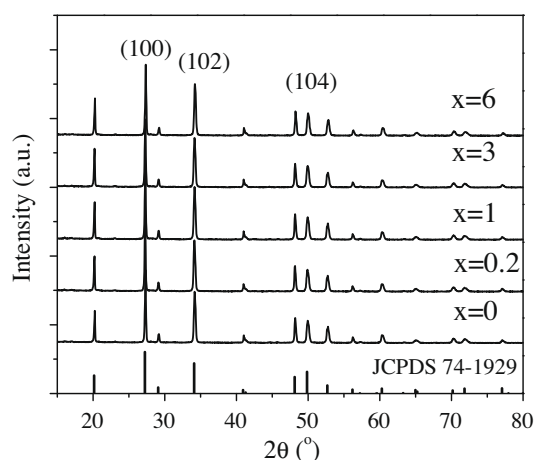


Fig. 1. XRD patterns of the $\text{YBO}_3:\text{Ce}^{3+}$ (1%), Yb^{3+} ($x\%$) ($x = 0, 0.2, 1, 3,$ and 6) and the reference data of JCPDS card Nos. 74–1929 for pure YBO_3 .

3. Results and discussion

Fig. 1 shows the XRD patterns of $\text{YBO}_3:\text{Ce}^{3+}$ (1%), Yb^{3+} ($x\%$) samples and the reference data of JCPDS Card No. 74-1929 for pure YBO_3 . As indexed in the figure, all diffraction peaks match well with those of pure hexagonal YBO_3 structure with lattice constants of $a = 0.3778$ nm and $c = 0.8814$ nm. The stronger diffraction peaks appear at 27.2°, 34.1°, and 49.8°, corresponding to the (1 0 0), (1 0 2), and (1 0 4) planes of YBO_3 crystals, respectively.

Luminescence measurements of Ce^{3+} and Yb^{3+} and decay curves of Ce^{3+} in $\text{YBO}_3:\text{Ce}^{3+}$, Yb^{3+} phosphors were investigated and gave a convincing evidence for the presence of Ce^{3+} to Yb^{3+} energy transfer. **Fig. 2** gives the photoluminescence (PL) and photoluminescence excitation (PLE) spectra of the samples with different Yb^{3+} doping concentrations. By monitoring the 5d to 4f transition of Ce^{3+} at 414 nm and ${}^2\text{F}_{5/2} \rightarrow {}^2\text{F}_{7/2}$ transition of Yb^{3+} at 973 nm, an intense and broad band was observed between 326 and 377 nm in the PLE spectra (**Fig. 2a**), which assigned to the 4f to 5d transition of Ce^{3+} . The observation of the Ce^{3+} 4f to 5d band in the excitation spectrum of Yb^{3+} shows that a CET process from Ce^{3+} to Yb^{3+} is theoretically possible.

Excitation at 358 nm light gave rise to emissions from both Ce^{3+} and Yb^{3+} ions, as shown in **Fig. 2b**. The broad bands center at 388 nm and 414 nm in the visible region of 370–480 nm have been assigned to the transition from the lowest 5d level to ${}^2\text{F}_{5/2}$ and ${}^2\text{F}_{7/2}$ of Ce^{3+} . The excited electronic configuration of Ce^{3+} is $5d^1$. The 5d electron of Ce^{3+} is not shielded from the surroundings and thus has a strong interaction with the neighboring anion ligands in the compounds. As a result, the excitation band of Ce^{3+} is broad and the excitation wavelength of Ce^{3+} can be tuned by the host materials. Moreover, it is worthy to note that a clear emission centered at 973 nm was also observed, corresponding to the ${}^2\text{F}_{5/2} \rightarrow {}^2\text{F}_{7/2}$ transition of Yb^{3+} ions. To prove the energy transfer from Ce^{3+} to Yb^{3+} , the Yb^{3+} single doped YBO_3 sample were also excited by 358 nm, however, we did not observe any peaks in rang from 900 nm to 1100 nm.

These results indicate that the emission of two NIR photons per absorbed one UV photon is possible with the Ce^{3+} – Yb^{3+} dual ions via a CET process. **Fig. 3** illustrates the schematic energy levels with transitions which may be involved in the CET process from one

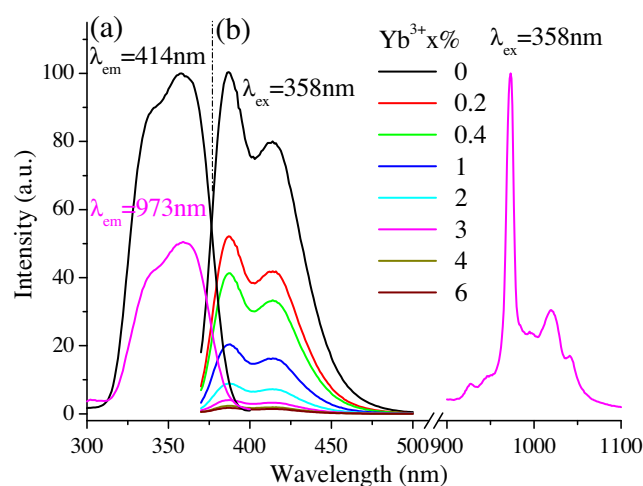


Fig. 2. (a) Photoluminescence excitation spectra of $\text{YBO}_3:\text{Ce}^{3+}$ (1%) sample ($\lambda_{\text{em}} = 414$ nm, Ce^{3+} : $5d \rightarrow 4f$ transition) and $\text{YBO}_3:\text{Ce}^{3+}$ (1%), Yb^{3+} (3%) sample ($\lambda_{\text{em}} = 973$ nm, Yb^{3+} : ${}^2\text{F}_{5/2} \rightarrow {}^2\text{F}_{7/2}$ transition); (b) Visible photoluminescence spectra of $\text{YBO}_3:\text{Ce}^{3+}$ (1%), Yb^{3+} ($x\%$) samples with different Yb^{3+} concentrations and NIR photoluminescence spectra of $\text{YBO}_3:\text{Ce}^{3+}$ (1%), Yb^{3+} (3%) sample ($\lambda_{\text{ex}} = 358$ nm, Ce^{3+} : $4f \rightarrow 5d$ transition).

Download English Version:

<https://daneshyari.com/en/article/1495518>

Download Persian Version:

<https://daneshyari.com/article/1495518>

[Daneshyari.com](https://daneshyari.com)